International Journal of Applied Engineering Research
ISSN 0973-4562 Volume 10, Number 7 (2015) pp. 16595-16612
© Research India Publications
http://www.ripublication.com

A High Voltage Gain DC-DC Converter With Voltage Multiplier Module For Photovoltaic System

S. Chandraleka and K. Sivapriya

M.E. Power Electronics and Drives
P.A. College of Engineering and Technology Pollachi, India
santhiyaleka@gmail.com
M.E. Power Electronics and Drives
P.A. College of Engineering and Technology Pollachi, India
sivapriya752@gmail.com

Abstract

The massive usage of fossil fuels worsens the environment and also it could not satisfy the energy demand. Nowadays the world pays attention to renewable energy sources such as photovoltaic sources fuel cells and wind energy and so on. Among them photovoltaic sources are predicted to become biggest energy sources in future due to clean efficient and environmental friendly performance. But the output of renewable energy system is low thus high step up dc to dc converters are mandatory for high efficiency. Here a high step up converter is proposed for a photovoltaic system. High step up gain without operating at an extreme duty ratio is achieved by a voltage multiplier module an asymmetrical interleaved high step up converter. The voltage multiplier module is consisting of both a conventional boost converter and coupled inductors. The boost converter is integrated into the first phase to obtain a considerably higher voltage conversion ratio. The two phase structure not only reduces the current stress through each power switch but also constrains the input current ripple that decreases the conduction losses of metal–oxide–semiconductor field effect transistors. A simulation model is developed in MATLAB to judge the performance of dc to dc converter.

Keywords— Boost–Flyback converter, High step-up, Photovoltaic system, Voltage multiplier module.

I. INTRODUCTION

Green power becomes more important due to global pollution problems. There exist many different types of renewable power technologies such as wind turbines, photovoltaic cells and fuel cells. Photovoltaic (PV) power-generation systems are now important and prevalent in distribution generation systems [1], [2]. Those systems transform light energy into electrical energy and convert low voltage into high voltage via a step-up converter which can convert energy into electricity using a grid-by-grid inverter or store energy into a battery set is shown in the Fig. 1. For example, in order to deliver the energy to a single-phase 220-V utility grid, a 380-V dc bus voltage is required with a full-bridge inverter [3], [4].

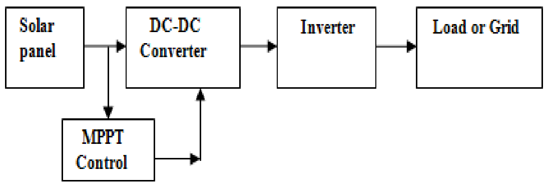

Fig. 1. Block diagram of pv system

Unfortunately the output voltage of the individual PV cells is lower than 40 V due to the safety and reliability issues in the household applications [4]. Large voltage conversion ratio of voltage gain is necessary for the frontend dc/dc converters. The output rectifier conducts only a very short time during each switching cycle with a high duty ratio. Thus resulting in serious reverse recovery problems and also the EMI problem is severe under this condition. The basic structure to obtain high conversion ratio is a cascade converter which has low efficiency and complexity. Another method is to use a transformer for stepping up the output voltage. In this case additional losses caused by the transformer and the switch are generated [7]. Theoretically conventional step-up converters such as flyback converter and the boost converter cannot achieve a high step-up conversion with high efficiency because of the resistances of elements or leakage inductance. The modified boost converter using inductor coupling is better compared to the conventional high boost converter [5], [6]. Despite these advances for high power applications conventional step up converters with a single switch are unsuitable and given an input large current ripple which increases conduction losses. Thus interleaved structures and asymmetrical interleaved structures are widely used. The current study also presents an asymmetrical interleaved converter for a high voltage gain and high power application [9].

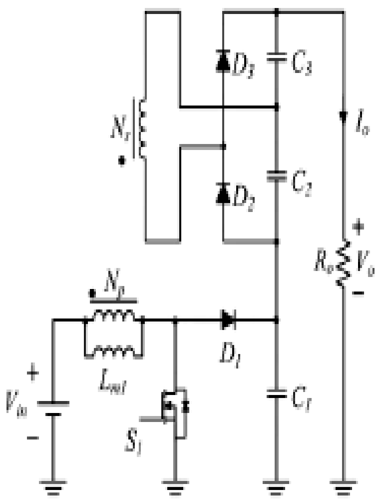

Fig. 2. Flyback-boost converter

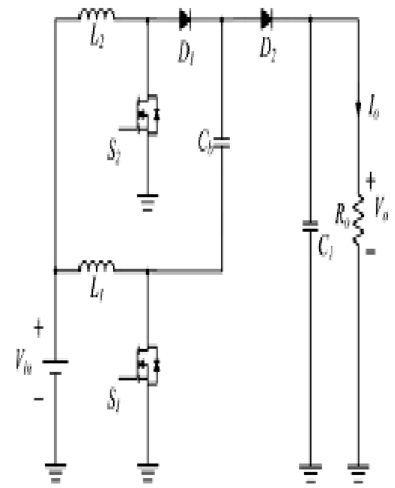

Fig. 3. Boost converter with voltage lift capacitor

The Fig. 2. shows the modified boost flyback converter is one of the simple approaches to achieving high step up gain via a coupled inductor. The leakage energy is recovered to the output terminal as the performance of the converter is similar to an active clamped flyback converter. An interleaved boost converter with a voltage lifts capacitor shown in Fig. 3. is similar to the conventional interleaved type. The other drawback of Solar PV systems is the variation in output voltage with variations in solar radiation and temperature. PV systems must be operated at a maximum power point (MPP) of specific current and voltage values so as to increase the PV efficiency [8]. One of such techniques is the use of Fuzzy Logic controllers in Maximum Power Point Tracking of the PV systems.

The Maximum power point tracking changes with the variation in the solar radiation and temperature so FLC is used to force the PV system to operate at the maximum power point. In this paper a highly robust Fuzzy Logic based controller is designed in MATLAB/Simulink environment. The FLC is used in Solar PV system along with a DC-DC converter to increase the efficiency of the Solar PV system. In the Fuzzy Logic Controller the modifications are done in Rule base and membership functions according to the variations in solar radiation and temperature. The output of the FLC is the change in the duty cycle of the DC-DC buck boost converter.

In the voltage multiplier module of the proposed converter the turns ratio of coupled inductors and voltage lift capacitor can be designed to extend voltage gain and it also offers an extra voltage conversion ratio [10]-[12].

Proposed converter has the following advantages:

1) Low input current ripple and low conduction losses making it preferable for high power applications.
2) The high step up voltage gain is achieved that renewable energy systems required.

3) Alleviates large voltage spikes on the main switch and leakage energy is recycled and fed to the output terminal.
4) The output voltage is greater than the main switch voltage stress of the converter
5) Low cost and high efficiency are attained.

II. CIRCUIT DESCRIPTION

The high step-up converter with voltage multiplier module is shown in Fig. 4(a). A conventional boost converter and two coupled inductors are located in the voltage multiplier module that is stacked on a boost converter to form an asymmetrical interleaved method. Primary windings of the coupled inductors with Np turns are used to decrease input current ripple and secondary windings of the coupled inductors with Ns turns are connected in series to extend voltage gain. The coupled inductors turns ratios are the same. The references of the coupling inductors are denoted by "." and "*" in Fig. 4(b).

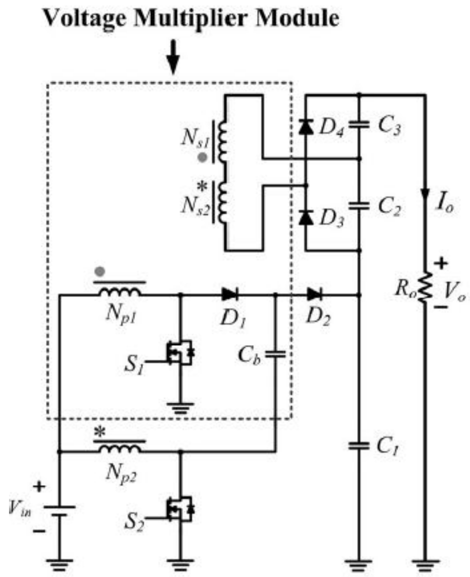

Fig. 4(a). Proposed high step-up converter with a voltage multiplier module

The equivalent circuit of the proposed converter is shown in Figure 3.4 where Lm1 and Lm2 are the magnetizing inductors L_{k1} and L_{k2} represent the leakage inductors S1 and S2 denote the power switches C_b is the voltage-lift capacitor and n is defined as a turns ratio Ns /Np.

The proposed converter operates in Continuous Conduction Mode (CCM) and the duty cycles of the power switches during steady operation are interleaved with a 180◦ phase shift the duty cycles are greater than 0.5.

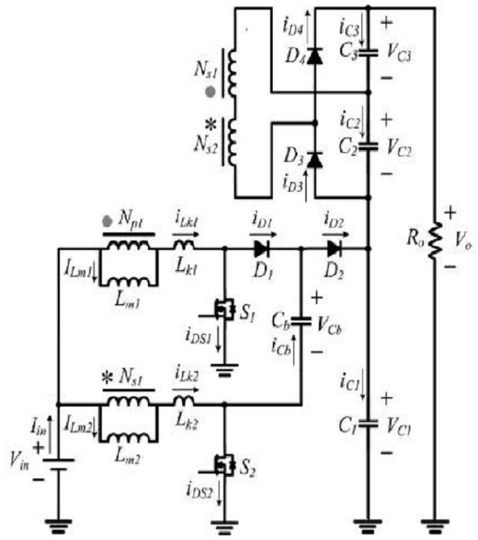

Fig. 4(b). Equivalent Circuit

III. MODAL ANALYSIS

The steady waveforms in one switching period of the proposed converter contain six modes.

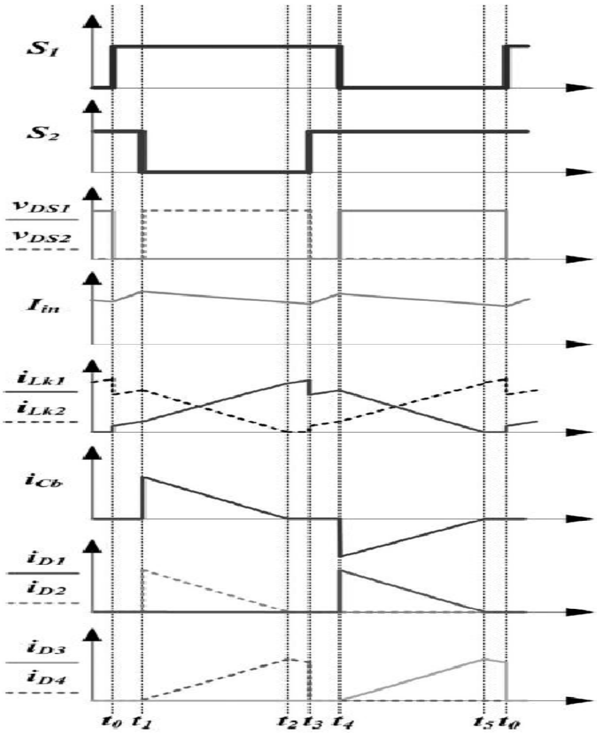

Fig. 5. Steady waveforms of the proposed converter

Mode 1 [t0, t1]: In mode1 operation at t=t0 the power switches s1 and s2 both are turned on. Now all the diodes d_1, d_2, d_3, d_4 are reversed biased. Magnetizing inductors L_{m1} and L_{m2} as well as leakage inductors L_{k1} and L_{k2} are linearly charged by the input voltage source V_{in}. The Fig. 6(a). shows the operation during mode1.

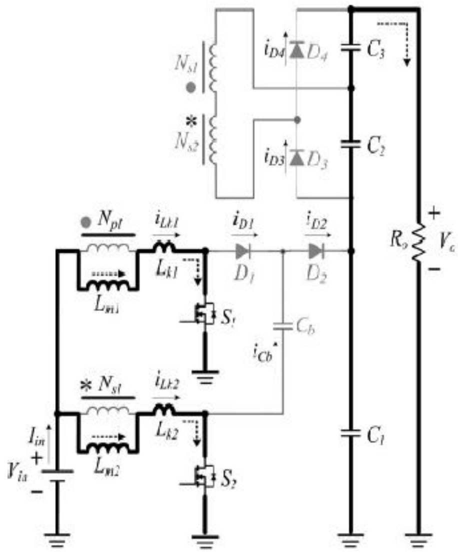

Fig. 6(a). Mode 1

Mode 2 [t1, t2]: During mode2 at t=t1 the power switch s2 is switched off thereby turning on the both diode d_2 and d_4. Magnetizing inductor is energized and the energy stored in L_{m2} is transferred to the secondary side charging the output capacitor C_3. The energy was released to the output capacitor C_1 via diode d_2 thereby extends the voltage on C_1that is fed from the input voltage source and magnetizing inductor L_{m2}, leakage inductor L_{k2} and voltage lift capacitor C_b. The Fig. 6(b). and show the operation during mode2.

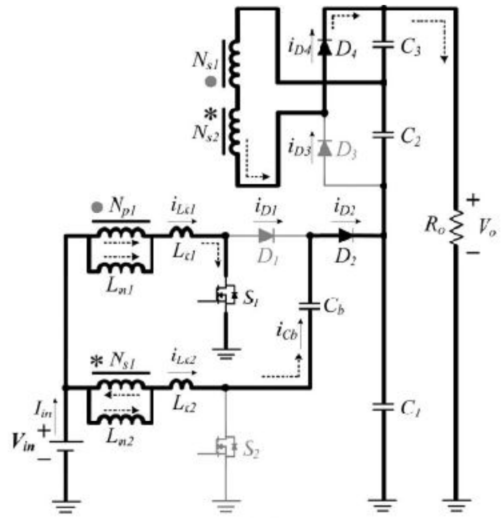

Fig. 6(b). Mode 2

Mode 3 [t2, t3]: In mode3 operation at t=t2 diode d_2 automatically switches off because the total energy of leakage inductor L_{k2} has been completely released to the filter capacitor C_1. Magnetizing inductor L_{m2} releases energy to the secondary side charging element output filter capacitor C_3 via diode d_4 until t3. The Fig. 6(c). shows the operation during mode3.

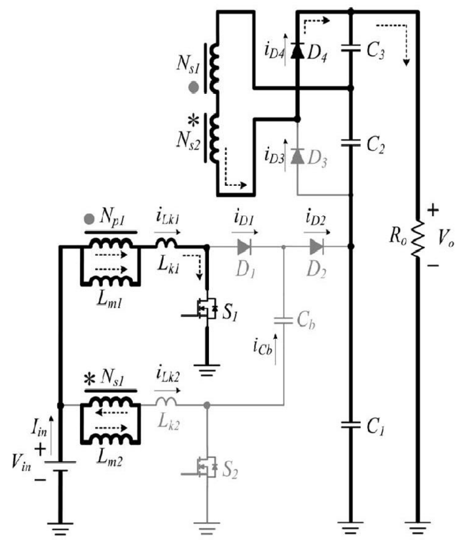

Fig. 6(c). Mode 3

Mode 4 [t3, t4]: In mode4 operation at t=t3 the power switch s2 is switched on and all the diodes are turned off. The operating states of modes 1 and 4 are one and the same. The Fig. 6(d). shows the operation during mode4.

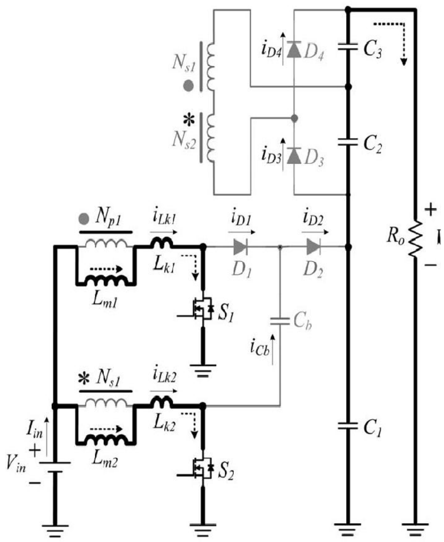

Fig. 6(d). Mode 4

Mode 5 [t4, t5]: In mode5 operation at t=t4 the power switch s1 is switched off that turns on both diode d_1 and d3. The energy that stored in magnetizing inductor L_{m1} is released to the secondary side charging the filter capacitor C_2. The input source and magnetizing inductor L_{m1} transfers the energy to voltage lift capacitor Cb via diode d1 that stores extra energy in C_b. The Fig. 6(e). shows the operation during mode5.

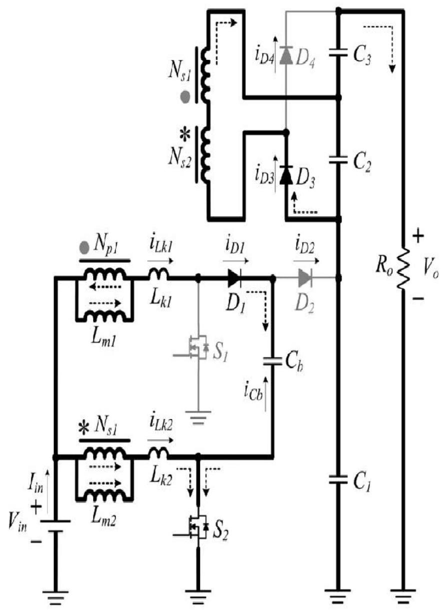

Fig. 6(e). Mode 5

Mode 6 [t5, t0]: In mode 6 operation at t=t5 diode D_1 is automatically turned off because the total energy of leakage inductor L_{k1} has been completely released to voltage lifting capacitor C_b. Magnetizing inductor Lm1 releases energy to the secondary side charging the output filter capacitor C_2 via diode D_3 until t0. The Fig. 6(f). shows the operation during mode6.

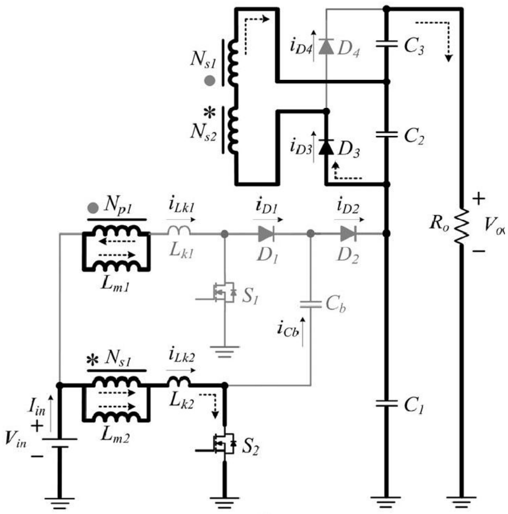

Fig. 6(f). Mode 6

IV. ANALYSIS DURING STEADY STATE

The analysis of the proposed converter in CCM for knowing circuit performance and the transient characteristics of circuitry is disregarded to simplify and some formulated assumptions are as follows:

1) In the proposed converter all of the components are ideal.
2) Neglecting Leakage inductors Lk1 and Lk2.
3) Because of infinitely large capacitance voltage VCb, VC1, VC2, and VC3 are considered to be constant.

A. VOLTAGE GAIN OF PROPOSED CONVERTER

Regarding as a conventional boost converter the first-phase converter voltage VCb can be given by the equation (1).

$$V_{cb}=V_{in}\frac{1}{1-D} \tag{1}$$

When switch S1 is turned ON and switch S2 is turned OFF voltage V_{c1}can be known by the equation (2).

$$V_{c1}=V_{in}\frac{1}{1-D}+V_{cb}=V_{in}\frac{2}{1-D} \tag{2}$$

The primary side energy transformation charges the output filter capacitors C2 and C3. When the switch S2 is in turn on state and the switch S1 is in turn-off state V_{c2} is equal to induced voltage of Ns1 and induced voltage of Ns2. When the switch S1 is in turn-on state and the switch S2 is in turn-off state V_{c3} is also equal to induced voltage of Ns1 and induced voltage of Ns2. Thus voltages Vc2 and Vc3 can be derive from the equation (3).

$$V_{c2} = V_{c3} = n.V_{in}.1 + \frac{D}{1-D} = \frac{n}{1-D}.V_{in} \quad (3)$$

The proposed converter output voltage can be derived from the equation (4).

$$V_o = V_{c1} + V_{c2} + V_{c3} = \frac{2n+2}{1-D}.V_{in} \quad (4)$$

The voltage gain of the proposed converter is

$$\frac{V_o}{V_{in}} = \frac{2n+2}{1-D} \quad (5)$$

The above equation (5) suggests that proposed converter has a high step-up voltage gain without having an extreme duty cycle.

B. VOLTAGE STRESSES ACROSS SEMI CONDUCTOR COMPONENTS

The voltage stress analyses of the components are done by ignoring the voltage ripples on the capacitors for simplification. The voltage stresses on power switches S1 and S2 are derived from the equation (6).

$$V_{s1} = V_{s2} = \frac{1}{1-D}V_{in} \quad (6)$$

The voltage stresses on power switches S1 and S2 account to the output voltage Vo with the turns ratio n can be denoted by the equation (7).

$$V_{s1} = V_{s2} = V_o - \frac{2n+1}{1-D}V_{in} \quad (7)$$

The voltage stress on diode D1 is equal to V_{c1} and the voltage stress on diode D2 is voltage$V_{c1} - V_{cb}$.These voltage stresses can be given by the equation (8) & (9).

$$V_{D1} = V_{c1} = \frac{2}{1-D}V_{in} \quad (8)$$

$$V_{D2} = V_{c1} - V_{cb} = \frac{1}{1-D}V_{in} \quad (9)$$

The voltage stresses on the diodes D1 and D2 account to the output voltage Vo can be expressed as by the equation (10) & (11).

$$V_{D1} = V_o - \frac{2n}{1-D}V_{in} \quad (10)$$

$$V_{D2} = V_o - \frac{2n+1}{1-D}V_{in} \quad (11)$$

The voltage stresses on the diodes D3 and D4 corresponds to the output voltage Vo can be expressed as by the equation (12).

$$V_{D3} = V_{D4} = \frac{2n}{1-D}V_{in} \quad (12)$$

Even though the voltage stresses on the diodes D3 and D4 rises as the turns ratio n increases the voltage stresses across the diodes D3 and D4 are always lower than the output voltage.

V. MAXIMUM POWER POINT TRACKING

Maximum power point has an important term in photovoltaic system because they maximize the output power from a PV system for a given set of conditions and thus maximize the array efficiency.

A. Perturb and Observation

The P&O is to create a perturbation by decreasing or increasing the duty cycle of boost converter and then observing the direction of change of PV output. If at any instant k, the output PV power P(k) & voltage V(k) Are greater than the previous computed power P(k-1) & voltage V(k-1) then the direction of perturbation is maintained otherwise it is reversed. The flow chart of the P&O algorithm is shown in Fig.7.

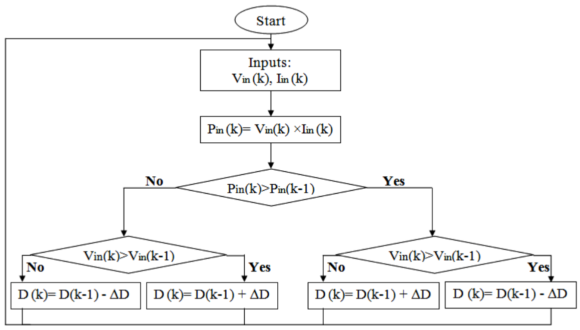

Fig. 7. Flow chart of P&O algorithm

Though the P&O algorithm is easy to proceed it has mainly the following drawbacks:

1) It cannot always operate at the maximum power point due to the slow trial and error process, and thus the maximum available solar energy from the PV arrays cannot be extracted all the time.
2) The PV system always operates in an oscillating mode which leads to the need of complicated input and output filters to absorb the harmonics generated.

B. **MPPT using Fuzzy Logic Control**

Fuzzy logic is one of the most powerful control methods. It is also known as multi rules based resolution and multivariable method. Fuzzy MPPT algorithm is well known for a decade. Fuzzy logic algorithm has the advantages of following factors imprecise inputs, no need to use of accurate mathematical model, and it can handle the nonlinearity. The flow chart of Fuzzy MPPT and Simulink model of proposed Fuzzy MPPT is as shown in Fig. 8 and Fig. 9.

It consists of two input variable and one output variable. The two FLC input parameter are the error (E), change in error (CE) and output parameter is duty cycle (D).

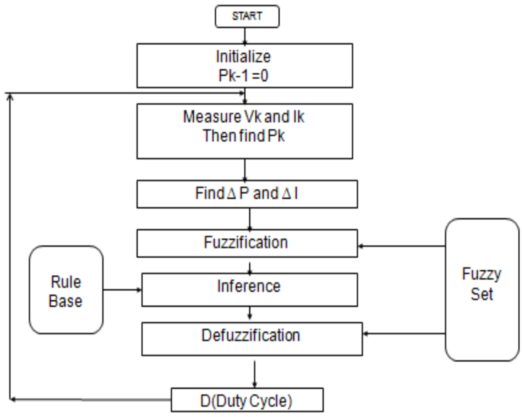

Fig. 8. Flow chart of fuzzy MPPT algorithm

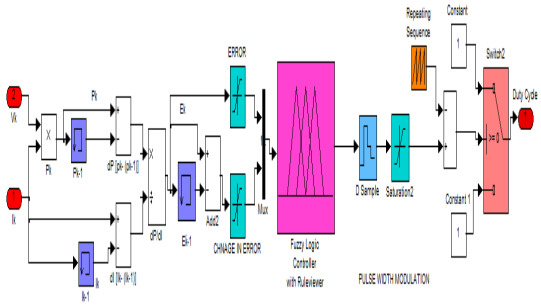

Fig. 9. Simulink of fuzzy MPPT

Using Fuzzy Logic parameter in MATLAB, membership functions and rule base are designed. Fig. 10(a)., Fig. 10.(b)., and Fig. 10(c). represent the graphical view of the triangular membership function for input variables error and change in error and output variable duty cycle of the fuzzy logic controller.

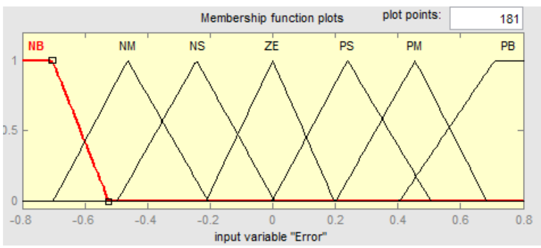

Fig. 10(a).

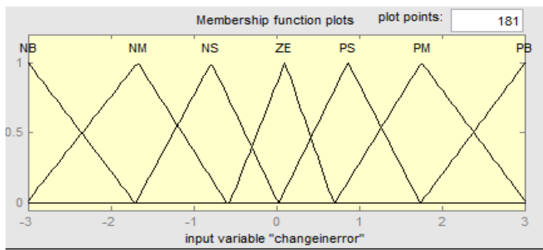

Fig. 10(b).

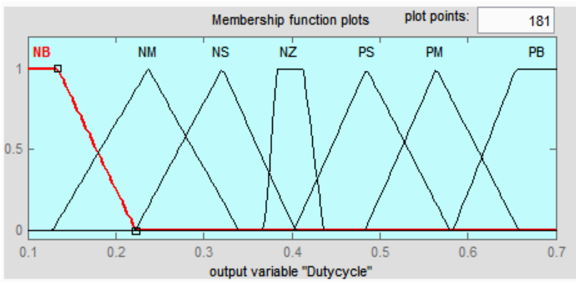

Fig. 10(c).

For the rule settings of fuzzy logic based MPPT, numerous number of subsets has been used. In the this case seven subsets and based on that forty nine rules have been used. The forty nine rules is quite time consuming for tuning but it represents better accuracy and dynamic response than previous method. The fuzzy rules are shown in Table. 1.

Table. 1. Rules of fuzzy

E/CE	NB	NM	NS	ZE	PS	PM	PB
NB	ZE	ZE	ZE	NB	NB	NB	NM
NM	ZE	ZE	ZE	NS	NM	NM	NM
NS	NS	ZE	ZE	ZE	NS	NS	NS
ZE	NM	NS	ZE	ZE	ZE	PS	PM
PS	PS	PM	PM	PS	ZE	ZE	ZE
PM	PM	PM	PM	ZE	ZE	ZE	ZE
PB	PB	PB	PB	ZE	ZE	ZE	ZE

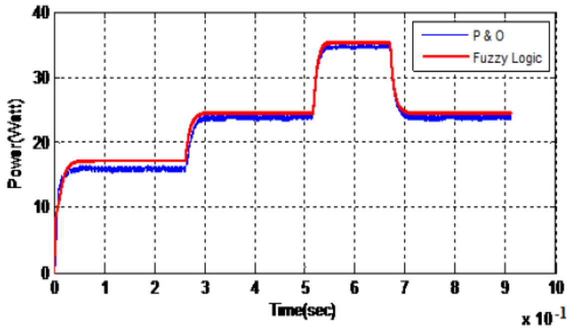

Fig. 11(a).

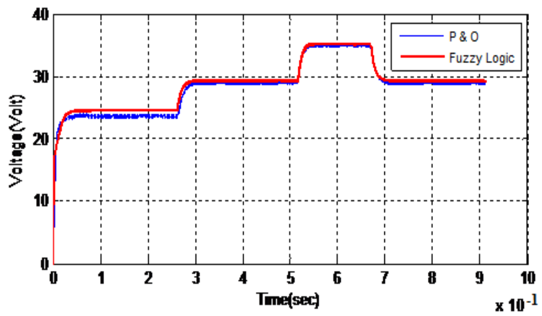

Fig. 11(b).

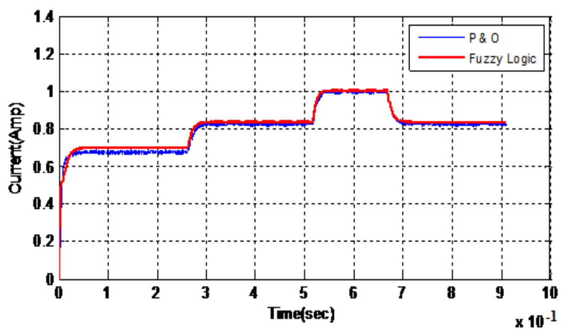

Fig. 11(c).

Fig. 11(a). shows the power curves which are tracked by fuzzy and P&O controllers Fig. 11(b). shows the voltage curves which are tracked by fuzzy and P&O controllers Fig. 11(c). shows the current curves which are tracked by fuzzy and P&O controllers. As shown power signal line smoothening, less oscillation and improved stable operating point than P&O is given by fuzzy controller.

VI. SIMULATION RESULTS

Table. 2. Parameters value

S. No.	Components	Symbol	Parameter
1	Magnetizing inductances	Lm1,Lm2	133uH
2	Leakage inductances	Lk1,Lk2	1.6uH
3	Capacitors	Cb, C2, C3	220uF
		C1	470uF
4	Input voltage		40V
5	Output voltage		373.1V

The table. 2. shows the values of parameters that are used in the simulation of high step up converter.

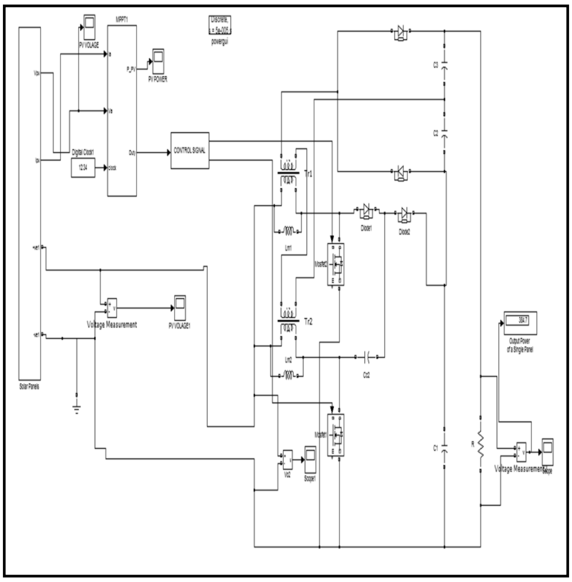

Fig. 12. Simulation Diagram of DC-DC Converter

The Simulink model of proposed step up converter with voltage multiplier module is shown in the Fig. 12. The Fig. 13(a). shows the input voltage and current waveform of photovoltaic source that was delivered to the dc to dc converter. This indicates output of solar panel is low and need to step up for higher value.

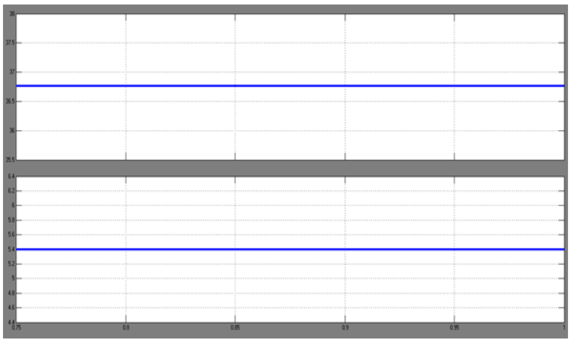

Fig. 13(a). Input Voltage and Current Waveform

The Fig. 13(b). shows the voltage and current waveform across switch1 in the dc to dc converter. Due to interleaved asymmetrical structure followed in the modified converter the stress across the switch is reduced that can be viewed from the waveform.

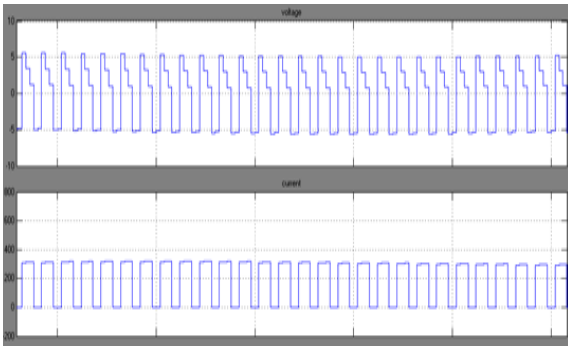

Fig. 13 (b). Stress across switch1

The Fig. 13(c). shows the voltage and current waveform across switch2 in the dc to dc converter. This shows stress across the switch is reduced that is lesser than output value.

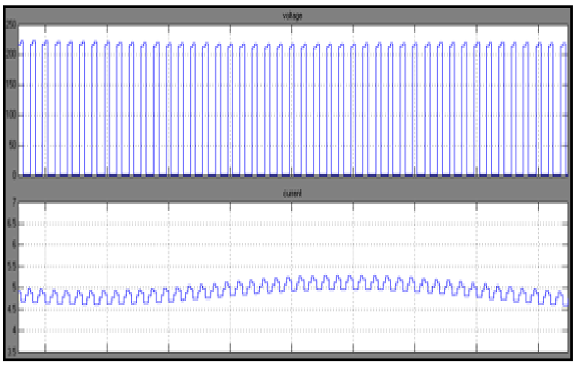

Fig. 13(c). Stress across switch2

The Fig. 13(d). shows the PWM signals for the switches S1 and S2. This tells that anyone switch will be in on state so it is continuous.

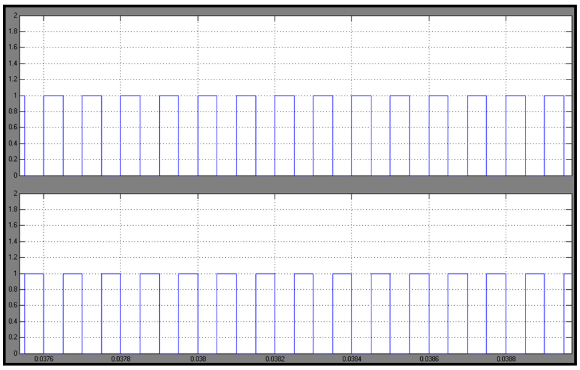

Fig. 13 (d). PWM Signals

The Fig. 13(e). shows the input current ripple waveform. From this it is clear that input ripple is reduced as interleaved asymmetrical structure is followed.

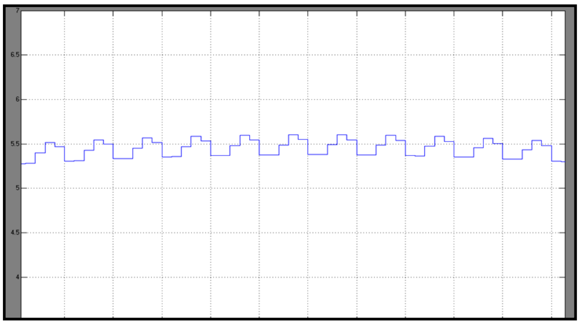

Fig. 13 (e). Input Current Ripple

The Fig. 13(f). shows the output voltage waveform of dc to dc converter. This tells that modified interleaved asymmetrical converter boosted the lower value to higher value several times with high efficiency.

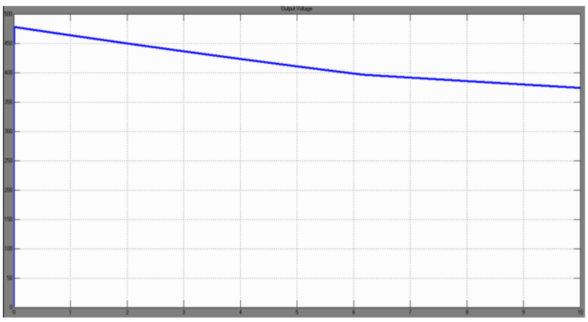

Fig. 13 (f). Output Voltage

VII. CONCLUSION

This paper has presented the analysis of steady state and experimental results for a proposed converter. The proposed converter with high step-up conversion without operating at an extreme duty ratio and a number of turns ratios through the voltage multiplier module and voltage clamp feature has been successfully implemented. The input current ripple across the power switch is constrained by approximately 6% as using of interleaved PWM scheme. The results indicate that leakage energy can be recycled through capacitor *Cb* to the output terminal. The voltage stresses over the power switches are reduced and are much lower than the output voltage (380 V). Thus switches conducted to low voltage rated and low on state resistance MOSFET can be selected.

REFERENCES

[1] G. K., Andersen, C.Klumpner, S. B. Kjaer, and F. Blaabjerg, "A newgreen power inverter for fuel cells," in Proc. IEEE 33rd Annu. Power Electron. Spec. Conf., 2002, pp. 727–733.

[2] Wuhua. Li and Xiangning. He, "Review of Nonisolated high-step-up DC/DC converters in photovoltaic grid-connected applications," IEEE Trans. Ind. Electron., vol. 58, no. 4, pp. 1239–1250, Apr. 2011.

[3] Kuo-Ching Tseng, Chi-Chih Huang, and Wei-Yuan Shih, "A High Step-Up Converter With a Voltage Multiplier Module for a Photovoltaic System," IEEE Transactions On Power Electronics, Vol. 28, No. 6, June 2013

[4] Wuhua Li, Weichen Li, Xiangning He, David Xu, and Bin Wu, "General Derivation Law of Nonisolated High-Step-Up Interleaved Converters With Built-In Transformer," IEEE Transactions On Industrial Electronics, Vol. 59, No. 3, March 2012

[5] Yi-Ping Hsieh, Jiann-Fuh Chen, Tsorng-Juu (Peter) Liang, and Lung-Sheng Yang, (2011), "Novel High Step-Up DC–DC Converter With Coupled-Inductor and Switched-Capacitor Techniques for a Sustainable Energy System," IEEE Transactions on Power Electronics, Vol. 26, No.12.

[6] Rong-Jong Wai, And Rou-Yong Duan (2005), "High Step-Up Converter With Coupled-Inductor," IEEE Transactions On Power Electronics, Vol. 20, No.5.

[7] Ju-Won Baek, Myung-Hyo Ryoo, Tae-Jin Kim, Dong-Wook Yoo, Jong-Soo Kim, "High Boost Converter Using Voltage multiplier," IEEE, Industrial Electric Research Center, 2005.

[8] Jan T., Bialasiewicz, "Renewable energy systems with photovoltaic power generators: Operation and modeling," IEEE Trans. Ind. Electron., vol. 55, no. 7, pp. 2752–2758, Jul. 2008.

[9] Rong-Jong Wai, Chung-You Lin, Rou-Yong Duan, and Yung-Ruei Chang,(2007), "High-Efficiency DC-DC Converter With High Voltage Gain and Reduced Switch Stress," IEEE Transactions on Industrial Electronics, Vol. 54, No.1

[10] Wuhu Li, Yi Zhao, Jeanne Wu, and Xiangning He, (2012), “Interleaved High Step-Up Converter With Winding-Cross-Coupled Inductors and Voltage Multiplier Cells,” IEEE Transactions on Power Electronics, Vol. 27, No.1.

[11] Wuhua Li, Yi Zhao, Yan Deng, and Xiangning He,(2010), “Interleaved Converter With Voltage Multiplier Cell for High Step-Up and High-Efficiency Conversion,” IEEE Transactions on Power Electronics, Vol. 25, No.9.

[12] Yungtaek Jang and Milan M. Jovanovic, “Interleaved Boost Converter With Intrinsic Voltage-Doubler Characteristic for Universal-Line PFC Front End,” IEEE Transactions On Power Electronics, Vol. 22, No. 4, July 2007.